J Therm Anal Calorim (2016) 126:205–224
DOI 10.1007/s10973-016-5695-0

Thermal, spectroscopic (IR, Raman, NMR) and theoretical (DFT) studies of alkali metal complexes with pyrazinecarboxylate and 2,3-pyrazinedicarboxylate ligands

G. Świderski[1] · H. Lewandowska[2] · R. Świsłocka[1] · S. Wojtulewski[3] · L. Siergiejczyk[3] · A. Wilczewska[3]

Received: 28 February 2016 / Accepted: 4 July 2016 / Published online: 23 July 2016

Abstract Pyrazinecarboxylic acid and its derivatives show biological properties (inter alia antimicrobial and antifungal). In the frame of this work, the salts of 2-pyrazinecarboxylic and 2,3-pyrazinedicarboxylic acids with alkali metal cations were synthesized as well as the spectroscopic (IR, Raman, NMR), theoretical [density functional theory (DFT)] and thermogravimetric studies of obtained compounds were done. The FT-IR and FT-Raman spectra of alkali metal 2-pyrazinecarboxylates and 2,3-pyrazinedicarboxylates were recorded and analyzed in the region of 4000–400 cm^{-1}. ^{1}H NMR and ^{13}C NMR spectra of analyzed compounds have been registered and assigned. The electronic charge distribution for the studied acids and their salts with lithium, sodium and potassium was calculated. All the calculations were done in the frame of DFT using 6-311++G(d,p) basis set. The thermal decomposition of the analyzed compounds was done.

Keywords Nicotinic acid derivatives · Pyrazinecarboxylates · Spectroscopy · Thermal analysis · DFT studies

✉ G. Świderski
swider30@gmail.com

[1] Division of Chemistry, Bialystok University of Technology, Wiejska 45E Street, 15-351 Białystok, Poland

[2] Centre for Radiobiology and Biological Dosimetry, Institute of Nuclear Chemistry and Technology, Dorodna 16, 03-195 Warsaw, Poland

[3] Institut of Chemistry, University of Bialystok, Ciolkowskiego Street 1K, 15-245 Białystok, Poland

Introduction

Pyrazines, also known as *p*-diazines (or 1,4-diazines, Scheme 1), are compounds containing a symmetrical (D_{2h}) aromatic heterocycle $C_4H_4N_2$. In nature, there are many substituted pyrazines that carry substituents at one or more of the four ring carbon atoms. The substituents include oxygenated functional groups like alkoxy groups and acyl groups or sulfur-containing thiol or sulfide groups. Only among alkylpyrazines (containing only carbon and hydrogen substituents) ca. 70 different compounds of that type have been identified in nature [1, 2]. The diversity of structures and roles pyrazine derivatives play in living organisms began to arouse the interest of researchers. The pyrazine derivatives have numerous prominent pharmacological effects: aspergillic acid, hydroxyaspergillic acid and other antibiotics of similar structure possess antibacterial activities [1–5]. Emimycin (3-hydroxypyrazine *N*-oxide), first isolated from *Streptomyces*, has been found a potent and selective inhibitor of the growth and nucleic acid synthesis in Toxoplasma gondii in human fibroblasts. Sulfonamides with pyrazine moiety are known to have high antibacterial activity [6]. Derivatives such as phenazine are well known for their antitumor, antibiotic and diuretic activities. Synthetic pyrazine derivatives exhibit a wide variety of pharmacological properties, including hypoglycemic [7–10] and diuretic [11–13] action. Pyrazinamide and its morpholino-methylene derivative act as tuberculostatic agents [14, 15]. Structural modifications of the pyrazine ring substituents in these compounds cause modulation in their biological activity [12, 16–20]. Nicotinic and isonicotinic amidrazones are also reported in the literature as antibacterial agents [16, 21]. They also act as diuretic [22] and antimycotic [23]. Tetramethylpyrazine (also known as ligustrazine) is reported to scavenge

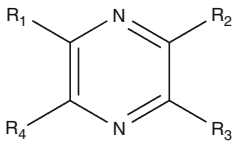

Scheme 1 General structure of diazines

superoxide anion and decrease nitric oxide production in human leukocytes [24]. For its active cardiovascular properties such as anti-platelet activity and free radical scavenging [25–27], ligustrazine has been used for the treatment of cardiovascular diseases (CVDs) in the clinic [28–30].

Pyrazines, synthesised chemically or biologically, are also used as flavoring additives. The pyrazine motif is observed in a large number of compounds that are responsible for the unique flavor and aroma of several foodstuffs and wines [31, 32]. Orally administered substituted pyrazines are rapidly absorbed from the gastrointestinal tract and excreted [33]. It is reported in the literature that absorption of pyrazine derivatives is optimal at intestinal pH (ca. 6–7) [3, 5]. The high incidence of pyrazine derivatives from the flavors of food systems and their effectiveness at very low concentrations has aroused a great interest in perfume industry [34]. Pyrazine ring is present in condensed azine dyes, for example, eurhodines, indulenes and safranines [35]. Nowadays, the pyrazine ring is a part of many polycyclic compounds of biological and/or industrial significance; examples are quinoxalines, phenazines and bio-luminescent natural products pteridines, flavins and their derivatives.

Compounds containing the quinoxaline fragment, such as Diquat, Propaquizafop and Quizalofop-ethyl, are very useful herbicides and have been used to control aquatic macrophytes [36]. While Diquat's activity consists mostly in its interaction with the photosystem I and via subsequent formation of free radicals, the two latter were shown to inhibit acetylCoA carboxylase [37, 38]. Nakamura et al. [39] synthesized sixty-six 2,3-dicyano-5-substituted pyrazines and measured their herbicidal activities against barnyard grass in pot tests to clarify the relationship between chemical structure and activity. The activity of 59 derivatives showed parabolic dependence on the hydrophobic substituent parameter at the 5-position of the pyrazine ring, indicating that the compounds should pass through a number of lipoidal–aqueous interfaces to reach a critical site for biological activity. It was found that the moiety of 2,3-dicyanopyrazine is essential for herbic ideal activity, and the 5-substituent on the pyrazine ring plays an important role in determining the potency of this activity and that para-substituted phenyl derivatives show undesirable effects on the potency of the activity at the ultimate site of herbicidal action. The results indicated that the structure of the substituted dicyanopyrazine moieties is an important function for the herbicidal activity and that the activity of these compounds is determined by the hydrophobic and steric parameters of substituents at the pyrazine ring. Similarly, Doležal et al. [40] prepared a series of substituted *N*-phenylpyrazine-2-carboxamides and diazachalcones. The most effective herbicide from the series was 6-chloro-*N*-(5-chloro-2-hydroxyphenyl)-pyrazine-2-carboxamide ($IC_{50} = 8$ μmol). The inhibitory activity of *ortho*-hydroxyl substituted derivatives was greater than that of their *para*-hydroxyl substituted isomers. An important lesson from the above mentioned studies comes from the fact that even subtle modifications of the studied pyrazine analogues have a high impact on the biological activity of a given compound. It is the time to conduct further studies aimed at rationalizing the biological activities found in order to develop more effective and clinically interesting compounds.

A renewed interest in the chemistry of pyrazine derivatives can be largely attributed to the major advances of chemotherapy, where heterocycles have been particularly prominent. Among the pyrazine-derived anticancer drugs, an epitome is a dipeptide Bortezomib, [(1R)-3-methyl-1-({(2S)-3-phenyl-2-[(pyrazin-2-ylcarbonyl)amino]propanoyl}amino)butyl] boronic acid, a 20S proteasome complex inhibitor that acts by disrupting various cell signaling pathways, thereby leading to cell cycle arrest, apoptosis and inhibition of angiogenesis. The hallmark of bortezomib action is the inhibition of NF-κB, thereby interfering with NF-κB-mediated cell survival, tumor growth and angiogenesis [41] and has been applied in the treatment of cancer [42]. In the study of Kamal et al. [43], a series of oxindole derivatives of imidazo[1,5-a]pyrazines were prepared and evaluated for their anticancer activity against a panel of 52 human tumor cell lines derived from nine different cancer types: leukemia, lung, colon, CNS, melanoma, ovarian, renal, prostate and breast. Among them one compound, namely 3-(E)-1-[3-(2-Fluorophenyl)imidazo[1,5-a]pyridin-1-yl]methylidene-2-indolinone, showed significant anticancer activity with GI_{50} values ranging from 1.54 to 13.0 μM. A series of fifty-one pyrazinyl derivatives have been synthesized by Rodrigues et al. [44] and evaluated for their activity against four cancer cell lines, exhibiting good cytotoxicity (IC_{50} ranging from 1.1 to 5.6 μg mL^{-1}). Structure–activity relationship (SAR) analysis indicated that the hydroxyl group located in *ortho* position is critical for the biological activity of these compounds. The presence of hydroxyl groups on benzene ring plays an important role in the anticancer activity of this series, feature especially observed in disubstituted derivatives. The mentioned instances on new pyrazine-derived drug development give a clear notion, how important for the successful research is understanding of the SAR analysis approach.

In the frame of our previous works, we studied the effect of over 40 metal cations on the electronic system, physicochemical and biological properties of different ligands—derivatives of benzoic [45–49] acids. The complexations of aromatic carboxylic acids by metal cations change the electronic charge distribution within the aromatic ring and the carboxylate anion. So far, our studies showed that the effect of metal cation on the electronic structure of pyridine ring of pyridinecarboxylic acids depends on the position of nitrogen atom within the carboxylic acid structure. In this work, the effect of alkali metal cations on the electronic structure of derivatives of pyrazine was studied. We have studied the salts of pyrazine 2-carboxylic acid (2PCA) and pyrazine 2,3-dicarboxylic acid (2,3PDCA) alkali metal salts. A range of complementary methods were used to determine the effect of alkali metals on the changes in the distribution of electronic charge in the pyrazine ring of the analyzed acids. As part of the work, we also investigated the impact of alkali metals on the (thermal stabilization) of the 2-pyrazinecarboxylic and 2,3-pyrazinedicarboxylic acids. These studies also allowed, along with the elementary analysis, to determine the degree of hydration of the tested salts.

Experimental and theoretical calculations

Sample preparation

The alkali metal salt of 2-pyrazinecarboxylic (2PCA) and 2,3-pyrazinedicarboxylic acids (2,3PDCA) was prepared by dissolving appropriate weighed amount of particular acids in hot aqueous solution of alkali metal hydroxides in a stoichiometric ratio ligand/metal—1:1 for 2-pyrazinecarboxylates and 1:2 for 2,3-pyrazinedicarboxylates. To 1 mmol of 2-PCA 10 cm^3 of 0.1 mol/L alkali metal hydroxide solution in water was added. The solutions were than heated in a shaker to ca 80°C for 1 h. Then, the solutions were left at RT for 24 h. Next, they were evaporated and dried at 50°C for 24 h. In order to obtain alkali metal salts with 2,3-pyrazinedicarboxylic acid, 0.1 mmol of acid was diluted in 20 mL of corresponding metal hydroxide (0.1 mol L^{-1}). Salts of 2,3-pyrazinedicarboxylate acid were prepared analogically.

Measurement and calculation

The FT-IR spectra were recorded with an Alfa (Bruker) spectrometer within the range of 400–4000 cm^{-1}. Samples in the solid state were measured in KBr matrix pellets and ATR technique. FT-Raman spectra of solid samples were recorded in the range of 400–4000 cm^{-1} with a MultiRam (Bruker) spectrometer. The resolution of the spectrometer was 1 cm^{-1}. The ^1H and ^{13}C NMR spectra of D_2O solution of studied compounds were recorded with a Bruker Avance II 400 MHz unit at room temperature. TMS was used as an internal reference. To calculate optimized geometrical structures of 2-pyrazinecarboxylic and 2,3-pyrazinecarboxylic acid and lithium, sodium and potassium salts, quantum–mechanical method was used: density functional (DFT) hybrid method B3LYP with non-local correlation provided by Lee–Young–Parr expression. All calculations were carried out with functional base 6-311++G(d,p). Calculations were performed using the Gaussian09 package [50]. Experimental spectra were interpreted in terms of calculated at DFT method in B3LYP/6-311++G(d,p) level and literature data [51]. Theoretical wavenumbers were scaled according to the formula: $\nu_{scaled} = 0.98 \cdot \nu_{calculated}$ for B3LYP/6-311++G(d,p) level method [52] Chemical shifts (δ_i) were calculated by subtracting the appropriate isotopic part of the shielding tensor (σ_i) from that of TMS (σ_{TMS}): $\delta_i = \sigma_{TMS} - \sigma_i$ (ppm). The isotropic shielding constants for TMS calculated using the DFT method at the same level of theory were equal to 31.8201 ppm and 182.4485 ppm for the ^1H nuclei and the ^{13}C nuclei, respectively. The electronic charge distribution was calculated with natural bond orbital (NBO) [53] at B3LYP/6-311++G(d,p) level of theory. The HOMA [54] and Bird I_6 [55] aromaticity indices were calculated for theoretical structures. The products of dehydration and decomposition processes were determined from the TG curves. Thermogravimetric analysis (TG) was performed on a Mettler Toledo Star TGA/DSC1 unit. Argon was used as a purge gas (20 mL min^{-1}). Samples between 2 and 4 mg were placed in aluminum pans and heated from 50 to 850 °C with a heating rate of 10 °C min^{-1}.

Results and discussion

Thermal study and elemental analysis

Alkali metal salts of the pyrazino 2-carboxylic acid 2,3-pyrazine dicarboxylic acids were dried for 24 h at 50 °C. The degree of hydration of the salt defined on the basis of thermogravimetric and elemental analysis was limited. Sodium, potassium and rubidium 2-pyrazinecarboxylates and sodium 2,3-pyrazinecarboxylate were anhydrous. For other salts, the degree of hydration ranged from 0.5 to 1.5 H_2O per molecule (Tables 1, 2; Fig. 1). Dehydration of the salts studied takes place in a single step (for all the hydrated salts). The press of thermal decomposition of both ligands is a single step press occurring at similar temperatures. 2,3-Pyrazinecarboxylic acid decomposes at about 210 °C, and 2-pyrazinecarboxylic acid at about 230 °C. Thermal decomposition of the salts studied takes place in several stages. The products of the first stage of the lithium salts decomposition are lithium carbonates and organic

Table 1 Elemental analysis and thermogravimetric analysis for lithium, sodium, potassium, rubidium and cesium 2-pyrazinecarboxylates

Compound[a]	Elemental analysis						Range of decomposition	Mass loss/%		Product decomposition
	Content C/%		Content H/%		Content N/%			Calc.	Exp.	
	Exp.	Calc.	Exp.	Calc.	Exp.	Calc.				
$Li_2L{\cdot}0.75H_2O$	41.1	41.79	3.13	2.90	18.52	19.51	80–110	95.91	96.70	Li_2L
							350–450	59.17	57.50	$Li_2CO_3 + C_{org}$
							550–850	25.75	22.50	Li_2CO_3
Na_2L	41.13	41.07	1.95	2.05	18.89	19.16	230–330	63.28	63.50	$Na_2CO_3 + C_{org}$
							850<	36.27	–	Na_2CO_3
K_2L	36.48	36.99	1.64	1.85	16.28	17.26	380–450	66.64	66.50	$K_2CO_3 + C_{org}$
							450–850	42.60	44.00	K_2CO_3
Rb_2L	28.10	28.77	1.25	1.44	12.26	13.42	440–490	73.61	72.50	$Rb_2CO_3 + C_{org}$
							490–850	55.36	55.50	Rb_2CO_3
$Cs_2L{\cdot}0.5H_2O$	23.26	22.63	1.40	1.51	10.62	10.56	220–250	96.61	96.65	Cs_2L
							330–430	78.25	78.50	$Cs_2CO_3 + C_{org}$

[a] L = 2PCA (ligand = 2-pyrazinecarboxylic acid)

Table 2 Elemental analysis and thermogravimetric analysis for lithium, sodium, potassium, rubidium and cesium 2,3-pyrazinedicarboxylates

Compound[a]	Elemental analysis						Range of decomposition	Mass loss/%		Product decomposition
	Content C/%		Content H/%		Content N/%			Calc.	Exp.	
	Exp.	Calc.	Exp.	Calc.	Exp.	Calc.				
$Li_2L{\cdot}0.75H_2O$	39.59	40.00	1.18	1.11	15.07	15.56	220–270	95.24	94.80	Li_2L
							350–450	74.38	74.50	$Li_2CO_3 + C_{org}$
							450–850	39.99	35.00	Li_2CO_3
Na_2L	33.81	33.95	0.96	0.94	12.66	13.20	410–460	78.26	81.00	$Na_2CO_3 + C_{org}$
$K_2L{\cdot}0.5H_2O$	27.40	28.42	0.97	1.18	9.72	10.05	50–100	96.58	96.85	K_2L
							350–490	81.13	80.00	$K_2CO_3 + C_{org}$
							490–800	54.56	55.00	K_2CO_3
$Rb_2L{\cdot}H_2O$	19.33	20.27	1.11	1.13	7.46	7.88	90–120	94.93	94.70	Rb_2L
							350–400	86.32	85.00	$Rb_2CO_3 + C_{org}$
							400–700	64.63	–	Rb_2CO_3
$Cs_2L{\cdot}1.5H_2O$	15.44	15.68	0.93	1.09	5.18	7.61	110–180	94.12	94.40	Cs_2L
							340–400	87.45	87.00	$Cs_2CO_3 + C_{org}$
							400–700	64.63	–	Cs_2CO_3

[a] L = 2,3PDCA (ligand = 2,3-pyrazinedicarboxylic acid)

carbon residues formed during the decomposition of the aromatic ring (Tables 1, 2; Figs. 1, 2). For both ligands, press takes place at the same temperature of 350–450 °C. Further heating of lithium salts leads to combustion of organic carbon residue. The final product of this decomposition step is lithium carbonate (at a temperature of about 850 °C for 2-pyrazinecarboxylate (Fig. 1) and 750 °C for 2,3-pyrazinedicarboxylate (Fig. 2). The sodium 2-pyrazinecarboxylic probably undergoes thermal decomposition into sodium carbonate at a temperature higher than 850 °C (outside the test temperature range). Intermediate product of this decomposition is a mixture of sodium carbonate and residual organic carbon from the decomposition of the pyrazine ring (this product is formed in the temperature range of 500–600 °C). Thermal decomposition of sodium 2,3-pyrazinedicarboxylate yields a mixture of sodium carbonate and organic carbon, which decompose to sodium carbonate at a temperature above 850 °C. The final decomposition product of potassium 2,3-pyrazinedicarboxylate is potassium carbonate (formed at a temperature above 800 °C). The intermediate product is a mixture of potassium carbonate and residual organic carbon from the decomposition of the pyrazine ring (this product is formed in the temperature range of 350–490 °C).

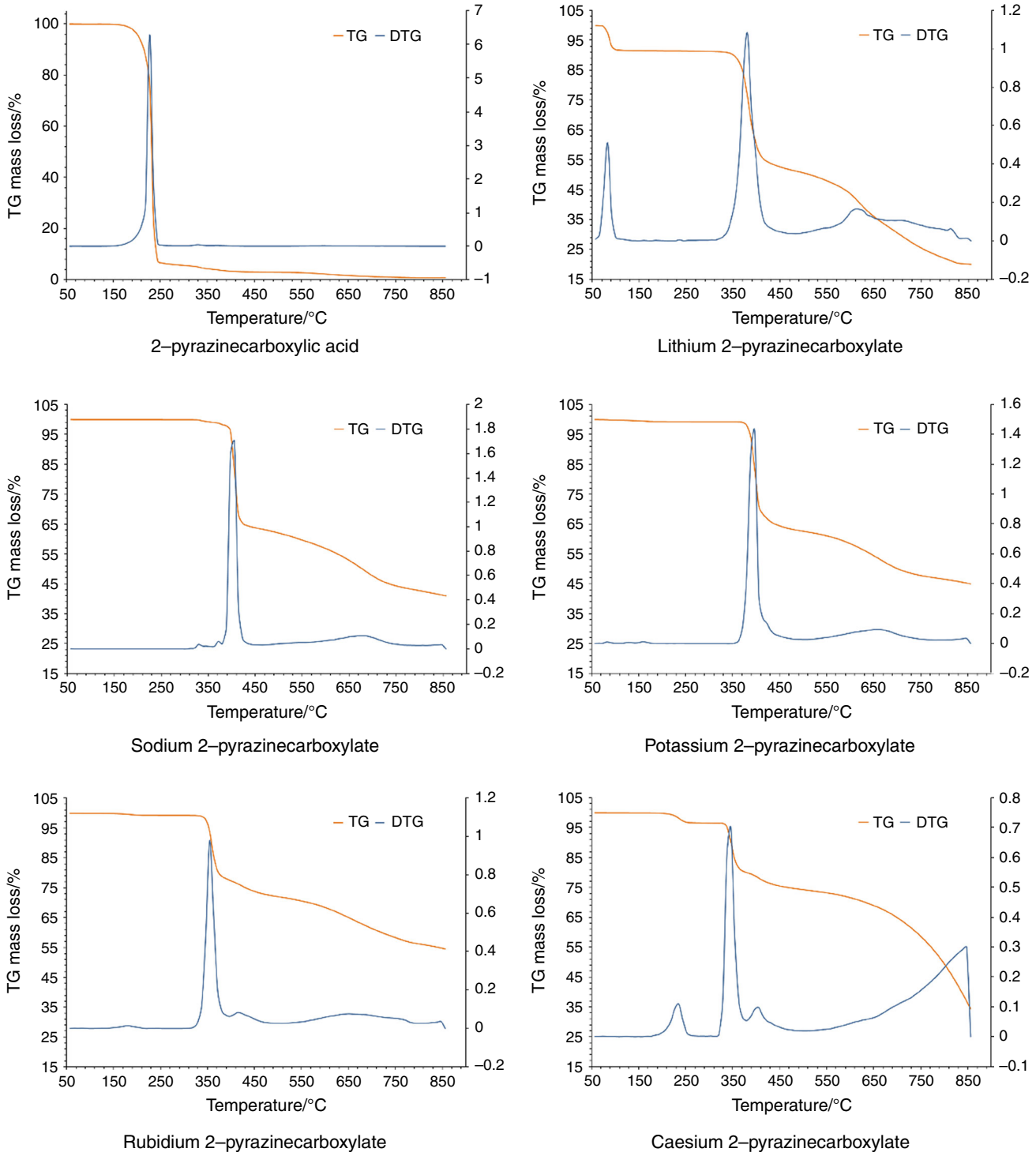

Fig. 1 Curves of thermal decomposition (*TG* and *DTG curves*) of alkali metal salts with 2-pyrazinecarboxylic acid (2PCA)—*left diagrams* and 2,3-pyrazinedicarboxylic acid (2,3PDCA)—*right diagrams*

In the case of potassium 2-pyrazinecarboxylate, the final product of degradation is potassium carbonate (at a temperature of 850 °C). An intermediate product is a mixture of potassium carbonate and organic carbon. The process of thermal decomposition of 2-pyrazinecarboxylate rubidium occurs in two stages. In the first stage taking place at a temperature of from 340 to 390 °C, a mixture of rubidium carbonate and organic carbon is formed (Fig. 1), and the second step yields rubidium carbonate (at a temperature of from 390 to 850 °C). The intermediate product of

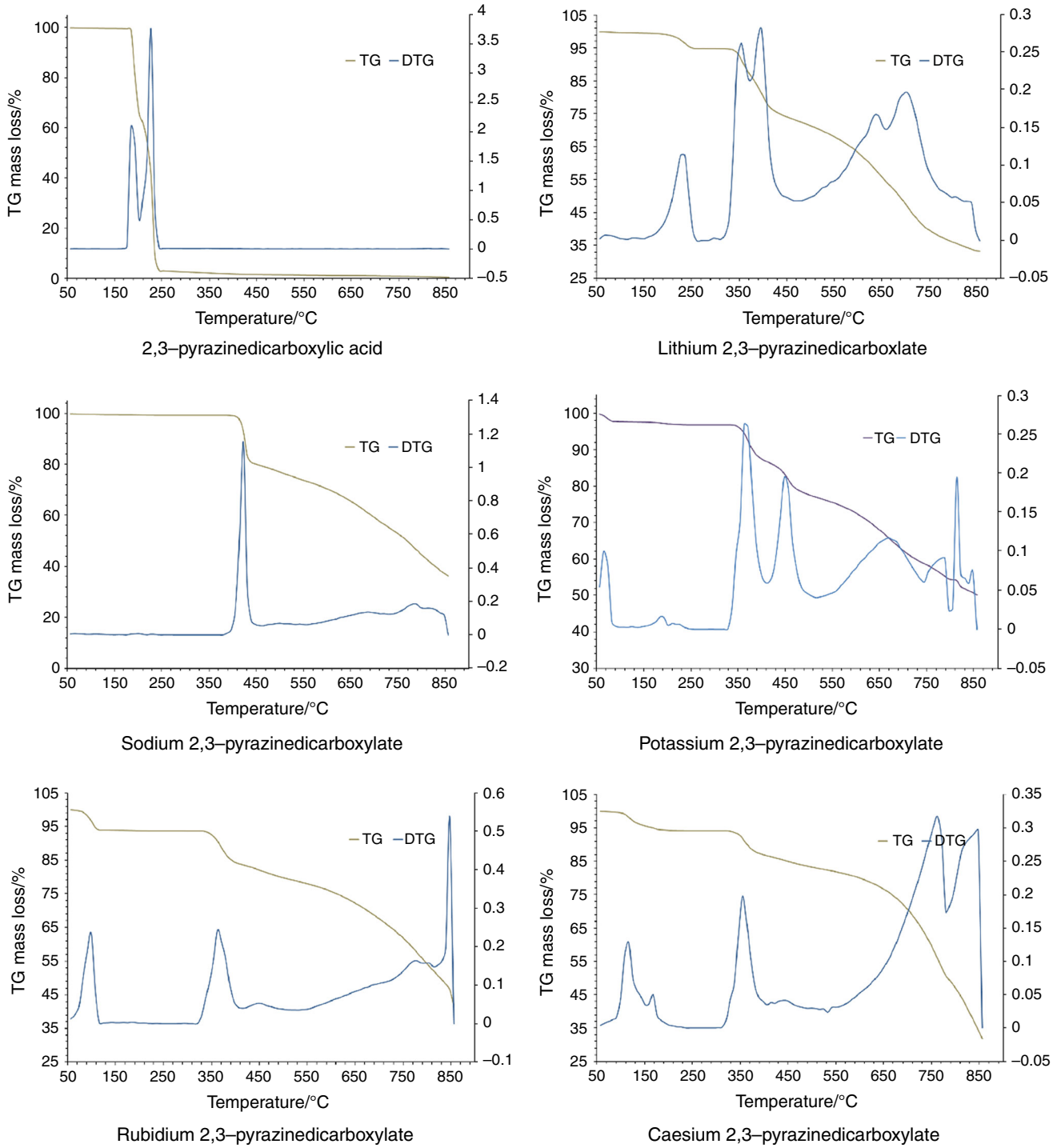

Fig. 2 Curves of thermal decomposition (*TG* and *DTG curves*) of alkali metal salts with 2,3-pyrazinedicarboxylic acid (2,3PDCA)

decomposition of rubidium 2,3-pyrazinedicarboxylate is a mixture of rubidium carbonate and residual organic carbon from the decomposition of the pyrazine ring (this product is formed in the temperature range of 350–400 °C). Further heating leads to unidentified products (Fig. 2).

The decomposition process of the cesium 2-pyrazinecarboxylate gives a mixture of cesium carbonate and carbon, which decomposes in the next step of heating, yielding probably the cesium oxide, Cs_2O.

Also, heating of cesium salt of 2,3-pyrazine dicarboxylic acid also gave a mixture of cesium carbonate and organic carbon; nevertheless, further heating leads to the formation of other products that could not be identified (unknown stable breakdown products—probably the cesium oxide, Cs_2O).

Comparing the curves of the thermal decomposition of the alkali metal salt of either acid, we observed that salts of 2-pyrazinecarboxylic acid decomposed at a slightly higher temperature than the salts of 2,3-pyrazinedicarboxylic acid. For all of the alkali metal salts of both ligands, thermal decomposition occurred yielding an intermediate product that was a mixture of alkali metal carbonate and organic carbon residues formed during decomposition of an aromatic acid. It was also observed that in the case of cesium salt, the carbonates formed were unstable and underwent further degradation at temperatures above 430 °C (2PCA acid salt) and above 700 °C (salt of 2,3PDCA).

IR and Raman study

Table 3 shows the wavenumbers and intensities of the bands present in IR spectra registered in the KBr matrix by ATR technique and as well those theoretically calculated by DFT (B3LYP-6-311++G**) and Raman spectra of 2-pyrazinecarboxylate and its salts with alkali metals. Table 4, in turn, shows the registered and calculated wavenumbers and intensities of the IR bands as well as the Raman spectra of 2,3-pyrazinedicarboxylate and alkali metal salts thereof. The experimental spectra were interpreted based on theoretical calculations and data presented in the literature [51]. The normal ring vibrations of aromatic acids and salts were assigned according to the Varsányi numbering [56]. Figure 3 shows the experimental spectrum recorded in KBr matrix and the Raman spectrum of 2-pyrazinecarboxylic acid and the chosen salt (of sodium). In the spectra of the salts, the characteristic vibrational bands of the carboxylate anion can be observed. These include asymmetric stretching vibration band of the carboxylate anion $\nu_{as}COO^-$ and symmetric stretching vibration band ν_sCOO^-. For the salts of 2-pyrazinecarboxylate upon the coordination of the carboxyl group the alkali metal cation, there appears a single band of $\nu_{as}COO^-$ vibration, present in the studied salts in the wavenumber range: 1619–1615 cm^{-1} (IR_{KBr}), 1631–1613 cm^{-1} (IR_{ATR}) and 1646–1617 cm^{-1} (Raman) and a single band of ν_sCOO^- vibration present in the range of 1389–1381 cm^{-1} (IR_{KBr}), 1385–1369 cm^{-1} (IR_{ATR}) and 1393–1382 cm^{-1} (Raman). There was also observed some single asymmetric and symmetric bending vibrations in the plane of the carboxylate anion $\beta_{as}COO^-$ and β_sCOO^- respectively at wavenumbers: 538–516 cm^{-1} (IR_{KBr}), 548–517 cm^{-1} (IR_{ATR}) and 547–512 cm^{-1} (Raman) and 855–848 cm^{-1} (IR_{KBr}), 854–840 cm^{-1} (IR_{ATR}) and 859–842 cm^{-1}. In the spectra of alkali metal 2-pyrazinecarboxylates, there were also observed the symmetrical out-of-plane bending vibrations of the carboxylate anion γ_sCOO^- in the ranges of: 807–795 cm^{-1} (IR_{KBr}), 797–786 cm^{-1} (IR_{ATR}) and 799–786 cm^{-1} (Raman). The coordination of the alkali metal atom by the carboxyl group induces the formation of the carboxylate anion and the change in electron charge distribution within that group. Along with the change in an alkali metal atom in the salt (in the series Li–Na–K–Rb–Cs) the charge distribution and the degree of metal–ligand binding as manifested by changes in wavenumbers bands derived from the carboxylate anion vibration ν_sCOO^- and $\nu_{as}COO^-$. Change in the ionic character of bond is associated with the increase or decrease in the disparity of ν_sCOO^- and $\nu_{as}COO^-$ band wavenumbers in the spectra of salt in the test series (parameter $\Delta\nu = \nu_{as}COO - \nu_sCOO^-$).

We observed a decrease in the $\Delta\nu$ the IR spectra are IR_{ATR}, IR_{KBr}, Raman spectra in the studied salts in the series Li–Na–K–Rb–Cs. In the case of the IR_{KBr} spectra, these changes were irregular in the studied series of metal salts. A similar effect was observed earlier in the case of alkali metal salts of other ligands, including 2-pyridinecarboxylic acid [57, 58]. We also observed the dependencies between some parameters of metals (including metal ion potential) and the values of the wavenumbers of carboxylate anion vibrations in the salts of the given metals with different ligands.

In the studied 2,3-pyrazinedicarboxylate alkali metal salts, the ratio of ligand to metal is 1:2. Both carboxyl groups of the ligand are substituted with an alkali metal. The spectra of these salts comprise each the two bands derived from symmetric stretching vibration ν_sCOO^- carboxylate anion and two bands derived from asymmetric stretching vibration carboxylate anion $\nu_{as}COO^-$ (Fig. 4; Table 4). $\nu_{as}COO^-$ vibration bands appear at wavenumbers: 1641–1613 and 1600–1588 cm^{-1} (IR_{KBr}), 1641–1612 and 1595–1585 cm^{-1} (IR_{ATR}) and 1631–1604 and 1604–1586 cm^{-1} (Raman). ν_sCOO^- vibration bands appear at wavenumbers: 1398–1388 and 1361–1351 cm^{-1} (IR_{KBr}), 1399–1389 and 1361–1351 cm^{-1} (IR_{ATR}) and 1401–1388 and 1366–1357 cm^{-1} (Raman). In the spectra of 2,3-pyrazinodicarboksylates of alkali metals, one can also observe two strands coming from asymmetric and symmetric in the plane bending vibrations of the carboxylate anion $\beta_{as}COO^-$ and β_sCOO^- and two symmetrical out-of-plane bending vibration bands of the carboxylate anion γ_sCOO^- (Table 4). The wavenumbers of bands coming from the carboxylate anion vibrations change irregularly in the studied series of metal salts. The observed changes in the parameter $\Delta\nu = \nu_{as}COO - \nu_sCOO^-$ for a series of 2,3-pyrazinedicarboxylates (Li–Na–K–Rb–Cs) are also irregular.

Analyzing the values of wavenumbers and intensities of the bands derived from the vibration of the aromatic ring in the salts of 2PCA and 2,3PDCA acids, one can find a number of characteristic differences as compared to the spectra of ligands. Some of the bands present in the spectra of acids disappear for salts. Wavenumbers and intensities of most of the bands decrease in the salts in relation to the ligand. The disappearance of the bands, decrease in the

Table 3 Wavenumbers (cm^{-1}), intensities and assignments of bands occurring in the IR (KBr, ATR and DFT) and Raman spectra of 2-pyrazinecarboxylic acid and lithium, sodium, potassium, rubidium and cesium 2-pyrazinecarboxylates

2-Pyrazinecarboxylic acid					Assignment	
IR KBr	IR ATR	Raman	IR theoret	Inten		
3434 m			3760	98.83	ν(OH)	
3094 m	3094 w	3096 w	3193	0.29	$\nu(CH)_{ar}$	7b
3065 s	3063 m	3069 vs	3172	29.37	$\nu(CH)_{ar}$	20a
3032 w		3031 vw	3155	0.60	$\nu(CH)_{ar}$	20b
2922 w	2916 vw				$\nu(CH)_{ar}$	
2801–2451	2805–2451				ν(OH)	
1731 s			1786	332.82	ν(C=O)	
1718 s	1718 s	1710 m			ν(C=O)	
					$\nu_{as}COO^{-}$	
1590 vw		1594 m			$\nu(CC)_{ar}$, $\nu(CN)_{ar}$	8a
1532 m	1531 w	1534 s	1580	1.47	$\nu(CC)_{ar}$, $\nu(CN)_{ar}$	8b
1486 w			1499	4.65	$\nu(CC)_{ar}$, $\nu(CN)_{ar}$, $\beta(CH)_{ar}$	19a
1443 w	1443 w	1465 w	1439	33.03	$\nu(CC)_{ar}$, $\nu(CN)_{ar}$, $\beta(CH)_{ar}$	19b
1394 s	1396 s	1399 w	1380	102.44	β(OH)	
					$\nu_{s}COO^{-}$	
1316 vs	1313 vs	1322 m	1319	1.73	ν(C–O)	
1275 s	1272 s	1282 m	1239	22.71	$\beta(CH)_{ar}$, $\nu(CC)_{ar}$, $\nu(CN)_{ar}$	9a
1175 s		1173 w	1222	73.36	$\nu(CC)_{ar}$, $\nu(CN)_{ar}$	14
1154 vs	1154 s	1160 w	1198	7.43	$\nu(CC)_{ar}$, $\nu(CN)_{ar}$	13
1056 s	1054 s	1054 m	1130	241.89	$\beta(CH)_{ar}$, $\nu(CC)_{ar}$, $\nu(CN)_{ar}$	18b
1018 s	1018 s	1019 vs	1069	19.05	$\beta(CH)_{ar}$	18a
					Ring def	
956 w	959 w	960 vw	976	0.48	$\gamma(CH)_{ar}$	5
889 m	888 m	892 w	883	6.59	$\gamma(CH)_{ar}$, $\gamma(NH)_{ar}$	11
					$\beta_{s}COO^{-}$	
821 m	820 m	825 m	817	9.44		
785 s	786 m	786 w	791	34.42	βCO	
					$\gamma_{s}COO^{-}$	
					Ring def	
					$\varphi(CC)_{ar}$, $\gamma(CH)_{ar}$	4
722 w	723 sh		748	19.55	α(CCC)	6a
711 m	708 m	711 w				
701 m						
643 m	644 m	643 w	675	55.90	α(CCC)	6b
501 m		510 w	598	101.24	γ(CO), γ(OH)	
					$\beta_{as}COO^{-}$	
440 m		448 vw	441	6.66	$\varphi(CC)_{ar}$	16b

Table 3 continued

2-Pyrazinecarboxylate															Assignment	
Lithium					Sodium					Potassium						
IR KBr	IR ATR	Raman	IR theoret	Inten	IR KBr	IR ATR	Raman	IR theoret	Inten	IR KBr	IR ATR	Raman	IR theoret	Inten		
															ν(OH)	
															$\nu(CH)_{ar}$	7b
3066 vw	3074 w	3066 s	3198	0.62	3076 w	3076 vw	3052 vs	3199	0.86	3067 w	3069 w	3056 s	3199	1.02	$\nu(CH)_{ar}$	20a
		3050 vs	3164	40.26	3021 vw	3021 vw	3017 w	3161	47.25	3011 w	3014 vw	3044 vs	3158	51.14	$\nu(CH)_{ar}$	20b
			3147	2.13	2947 vw		2945 w	3142	3.72	2937 vw		2934 w	3139	4.93	$\nu(CH)_{ar}$	
															ν(OH)	
															ν(C=O)	
															ν(C=O)	
1616 vs	1631 s	1646 w	1567	221.77	1615 vs	1613 vs	1646 w	1619	235.44	1619 vs	1616 vs	1635 w	1624	297.70	$\nu_{as}COO^-$	
1575 vs	1575 m	1581 s	1615	114.36	1572 s	1573 m	1579 m	1572	196.27	1572 s	1570 m	1575 m	1596	124.17	$\nu(CC)_{ar}$, $\nu(CN)_{ar}$	8a
1527 m	1524 w	1526 s	1585	132.30	1522 w	1520 w	1523 m	1572	58.35	1520 m	1515 w	1521 m	1572	28.48	$\nu(CC)_{ar}$, $\nu(CN)_{ar}$	8b
1483 m	1480 w	1480 w	1501	13.33	1477 vw	1478 w	1482 w	1497	1.89	1471 w	1467 w	1474 w	1495	1.65	$\nu(CC)_{ar}$, $\nu(CN)_{ar}$, $\beta(CH)_{ar}$	19a
1422 s	1423 m	1432 m	1412	155.87	1422 s	1418 m	1428 s	1422	37.50	1408 vs	1403 m	1411 s	1418	14.29	$\nu(CC)_{ar}$, $\nu(CN)_{ar}$, $\beta(CH)_{ar}$	19b
															β(OH)	
1384 vs	1378 vs	1386 m	1437	202.13	1389 s	1385 s	1393 w	1403	291.72	1384 vs	1376 s	1386 m	1398	368.41	ν_sCOO^-	
															ν(C–O)	
1293 w	1294 vw	1297 w	1314	2.82	1262 vw	1265 vw	1241 vw	1312	3.33	1248 w	1245 w	1249 vw	1310	4.33	$\beta(CH)_{ar}$, $\nu(CC)_{ar}$, $\nu(CN)_{ar}$	9a
1185 s	1184 sh	1187 w	1228	12.37	1188 w	1188 w	1189 sh	1225	9.39	1181 m	1181 w	1181 sh	1224	8.73	$\nu(CC)_{ar}$, $\nu(CN)_{ar}$	14
1163 s	1163 m	1164 w	1196	13.32	1161 m	1161 m	1168 w	1194	14.92	1157 s	1156 m	1158 w	1192	13.32	$\nu(CC)_{ar}$, $\nu(CN)_{ar}$	13
1055 s	1055 m	1052 s	1192	29.50	1055 m	1056 m	1056 m	1090	31.64	1051 s	1049 m	1052 m	1189	32.05	$\beta(CH)_{ar}$, $\nu(CC)_{ar}$, $\nu(CN)_{ar}$	18b
1030 s	1030 s	1033 vs	1071	8.77	1020 m	1021 m	1023 s	1072	8.83	1020 s	1018 m	1021 s	1072	9.02	$\beta(CH)_{ar}$	18a
			1035	23.18				1035	22.27				1034	21.48	Ring def	
	966 vw	956 vw	992	0.28	998 vw	990 vw		989	0.45	989 vw	997 w		988	0.65	$\gamma(CH)_{ar}$	5
889 m		888 sh	887	4.87	878 w	878 w	884 w	889	4.42	874 m	875 w	875 w	896	4.24	$\gamma(CH)_{ar}$, $\gamma(NH)_{ar}$	11
855 m	840 m	859 m	883	31.06	855 m	854 m	853 m	870	26.73	848 s	845 m	848 s	860	41.38	β_sCOO^-	
837 m					827 vw	830 vw					824 vw					
															βCO	
807 m	794 m	798 w	802	27.58	797 m	797 m	799 w	807	26.51	796 s	796 m	798 w	809	24.54	γ_sCOO^-	
			761	32.90				754	20.16				748	32.90	Ring def	
767 vw			750	3.36	770 vw	768 w		750	2.21		758 w		749	1.62	$\varphi(CC)_{ar}$, $\gamma(CH)_{ar}$	4
727 m	725 m	734 w			735 w	736 m	736 m			735 m	734 m	732 m			α(CCC)	6a
					671 vw	694 vw				663 vw	697 vw					
633 m	647 m	630 w	636	54.19		633 w	620 w	631	0.49		643 w	620 w	630	0.65	α(CCC)	6b
															γ(CO), γ(OH)	
538 w	541 w	547 w	521	0.08	521 w	523 m	526 w	514	6.32	516 w	522 m	514 w	512	5.47	$\beta_{as}COO^-$	
432 m		439 vw	454	30.23	428 m		425 vw	455	27.24	433 s			454	25.23	$\varphi(CC)_{ar}$	16b

Table 3 continued

2-Pyrazinecarboxylate						Assignment	
Rubidium			Cesium				
IR KBr	IR ATR	Raman	IR KBr	IR ATR	Raman		
3068 w	3066 vw	3058 s	3068 m	3062 vw	3058 vs	$\nu(CH)_{ar}$	20a
3011 vw			3009 w	3005 vw	3006 w	$\nu(CH)_{ar}$	20b
2934 vw		2929 w	2936 w		2923 w	$\nu(CH)_{ar}$	
1619 vs	1613 vw	1627 w	1617 vs	1616 vs	1629 w	$\nu_{as}COO^-$	
1571 s	1569 m	1571 m	1573 vs	1572 m	1575 m	$\nu(CC)_{ar}$, $\nu(CN)_{ar}$	8a
1520 w	1514 w	1521 m	1520 m	1518 w	1521 m	$\nu(CC)_{ar}$, $\nu(CN)_{ar}$	8b
1464 w	1461 w	1471 w	1471 w	1466 w	1467 w	$\nu(CC)_{ar}$, $\nu(CN)_{ar}$, $\beta(CH)_{ar}$	19a
1405 s	1402 sh	1405 s	1406 vs		1401 m	$\nu(CC)_{ar}$, $\nu(CN)_{ar}$, $\beta(CH)_{ar}$	19b
1381 vs	1374 s	1382 m	1384 vs	1369 s	1386 m	$\nu_{sym}COO^-$	
1245 w	1243 w		1246 vw	1233 w		$\beta(CH)_{ar}$, $\nu(CC)_{ar}$, $\nu(CN)_{ar}$	9a
1180 sh	1178 sh		1181 m	1183 sh	1179 w	$\nu(CC)_{ar}$, $\nu(CN)_{ar}$,	14
1157 m	1156 m	1156 m	1157 s	1156 m	1160 vw	$\nu(CC)_{ar}$, $\nu(CN)_{ar}$	13
1051 m	1047 m	1048 m	1051 s	1048 m	1048 m	$\beta(CH)_{ar}$, $\nu(CC)_{ar}$, $\nu(CN)_{ar}$	18b
1018 m	1017 m	1019 s	1020 s	1020 m	1021 m	$\beta(CH)_{ar}$	18a
990 vw	995 vw		989 w	997 vw		$\gamma(CH)_{ar}$	5
874 w	874 w	873 w	874 m	868 w	869 w	$\gamma(CH)_{ar}$, $\gamma(NH)_{ar}$	11
848 m	844 m	846 s	848 s	840 m	842 m	β_sCOO^-	
795 m	794 m	798 w	796 s	786 m	786 w	γ_sCOO^-	
734 m	732 m	730 w	735 m	728 m	726 w	$\alpha(CCC)$	6a
673 w	701 w					$\alpha(CCC)$	6b
517 w	548 w	512 vw	517 w	517 vw	531 vw	$\beta_{as}COO^-$	
433 m			433 s			$\varphi(CC)_{ar}$	16b

Band intensity: *s* strong, *m* medium, *w* weak, *vw* very weak, *sh* shoulder; type of vibrations: *v* stretching, *β* bending in-plane, β_{ring} ring bending in-plane, *γ* bending out-of-plane, *α* ring bending, *φ* ring deformation, *sym* symmetric, *as* asymmetric

Table 4 Wavenumbers (cm^{-1}), intensities and assignments of bands occurring in the IR (KBr, ATR and DFT) and Raman spectra of 2,3-pyrazinedicarboxylic acid and lithium, sodium, potassium, rubidium and cesium 2,3-pyrazinedicarboxylates

2,3-Pyrazinedicarboxylic acid						
IR KBr	IR ATR	Raman	IR theoret	Inten		
3266 s	3264 m	3264 w	3759	108.57	ν(OH)	
			3746	94.50	ν(OH)	
3090 w	3097 vw	3098 s	3177	25.17	$\nu(CH)_{ar}$	20a
		3077 m	3161	0.23	$\nu(CH)_{ar}$	20b
2854–2500					ν(OH)	
1753 vs	1750 s		1821	335,00	ν(C=O)	
1719 vs	1715 vs	1725 vs	1791	299.02	ν(C=O)	
					$\nu_{as}COO^-$	
					$\nu_{as}COO^-$	
1691 s	1689 s	1687 m	1592	7.59	$\nu(CC)_{ar}$, $\nu(CN)_{ar}$	8a
1576 m	1579 m	1579 s	1583	13.59	$\nu(CC)_{ar}$, $\nu(CN)_{ar}$	8b
1539 w	1541 w	1542 vs	1478	7.93	$\nu(CC)_{ar}$, $\nu(CN)_{ar}$, $\beta(CH)_{ar}$	19a
1445 s	1444 m		1449	29.07	$\nu(CC)_{ar}$, $\nu(CN)_{ar}$, $\beta(CH)_{ar}$	19b
1396 m	1396 w		1388	118.32	β(OH)	
1360 s	1357 m	1355 w			β(OH)	
					ν_sCOO^-	
					ν_sCOO^-	
1268 vs	1262 s	1264 m			ν(C–O)	
1215 m	1209 m		1358	56.15	$\beta(CH)_{ar}$, $\nu(CC)_{ar}$, $\nu(CN)_{ar}$	9a
1180 s	1184 m	1183 m	1265	11.21	$\beta(CH)_{ar}$, $\nu(CC)_{ar}$, $\nu(CN)_{ar}$	18a
	1161 w		1233	12.35	$\nu(CC)_{ar}$, $\nu(CN)_{ar}$	14
1099 vs	1098 vs	1096 w	1195	251.09	$\nu(CC)_{ar}$, $\nu(CN)_{ar}$	13
			1147	163.75	$\nu(CC)_{ar}$, $\nu(CN)_{ar}$	
1064 w	1058 w	1064 s	1089	232.89	$\nu(CC)_{ar}$, $\nu(CN)_{ar}$	
994 w	993 vw	994 w	1083	7.89	$\beta(CH)_{ar}$	18b
938 w	935 w		995	0.05	$\gamma(CH)_{ar}$	5
					Ring def	
872 s	870 s	869 m	890	14.02	$\gamma(CH)_{ar}$, $\gamma(NH)_{ar}$	11
					β_sCOO^-	
834 w	836 m	836 w	853	11.29	$\gamma(CH)_{ar}$, $\gamma(NH)_{ar}$	
790 s	793 m	784 s	781	62.04	βCO	
731 w	738 w	740 w	756	29.88	$\varphi(CC)_{ar}$, $\gamma(CH)_{ar}$	4
					γ_sCOO^-	
685 m	678 s	680 w	661	73.97	α(CCC)	1
643 w	643 w	645 w	604	105.44	γ(CO), γ(OH)	
586 w		589 vw	600	6.22	$\varphi(CC)_{ar}$, $\gamma(CH)_{ar}$	16a
540 m		539 w	520	16.74		6a
					$\beta_{as}COO^-$	
431 w			430	2.40	$\varphi(CC)_{ar}$	16b

Table 4 continued

2,3-Pyrazinedicarboxylate																
Lithium					Sodium					Potassium						
IR KBr	IR ATR	Raman	IR theoret	Inten	IR KBr	IR ATR	Raman	IR theoret	Inten	IR KBr	IR ATR	Raman	IR theoret	Inten		
															ν(OH)	
															ν(OH)	
3082 vw		3081 vs	3166	41.18				3162	45.33				3154	54.00	$\nu(CH)_{ar}$	20a
3056 vw		3058 m	3149	0.97	3062 vw		3062 vs	3142	4.35	3059 vw		3062 vs	3129	12.99	$\nu(CH)_{ar}$	20b
															ν(OH)	
															ν(C=O)	
															ν(C=O)	
1626 vs	1626 vs	1630 w	1609	476.75	1641 vs	1641 m	1613 m	1697	596.52	1620 vs	1622 sh	1331 w	1681	737.02	$\nu_{as}COO^-$	
1600 vs	1595 vs	1596 vw	1600	229.04	1589 vs	1589 vs	1586 vw	1538	517.99	1588 vs	1589 vs	1604 w	1641	472.18	$\nu_{as}COO^-$	
			1579	70.54				1586	17.02				1584	14.77	$\nu(CC)_{ar}$, $\nu(CN)_{ar}$	8a
1562 s	1561 m	1563 s	1566	197.97	1558 sh	1558 m	1559 m	1564	2.46		1561 sh	1559 m	1562	3.23	$\nu(CC)_{ar}$, $\nu(CN)_{ar}$	8b
	1539 vw	1532 m	1496	57.24			1532 m	1479	27.94		1529 vw	1527 s	1476	27.02	$\nu(CC)_{ar}$, $\nu(CN)_{ar}$, $\beta(CH)_{ar}$	19a
1447 m	1454 m	1446 s	1379	15.22	1449 s	1443 m	1446 vs	1370	75.91	1432 s	1433 m	1434 vs	1368	100.54	$\nu(CC)_{ar}$, $\nu(CN)_{ar}$, $\beta(CH)_{ar}$	19b
															β(OH)	
															β(OH)	
1398 vs	1399 s	1401 m	1452	193.76	1389 s	1391 m	1390 m	1434	106.28	1389 s	1392 m	1390 m	1427	125,05	ν_sCOO^-	
1351 s	1358 s	1361 m	1387	327,44	1362 s	1361 s	1366 m	1378	304.53	1354 vs	1351 s	1357 m	1379	269.07	ν_sCOO^-	
															ν(C–O)	
1204 m	1205 w	1204 m			1198 m	1201 w	1201 m			1201 m	1211 vw	1206 m			$\beta(CH)_{ar}$, $\nu(CC)_{ar}$, $\nu(CN)_{ar}$	9a
1173 m	1170 m	1168 w	1255	1.66	1166 m	1167 w	1168 w	1253	9.42	1160 m	1157 m	1158 w	1251	8.46	$\beta(CH)_{ar}$, $\nu(CC)_{ar}$, $\nu(CN)_{ar}$	18a
	1141 w		1226	33.45		1140 vw		1217	32.59				1220	23.66	$\nu(CC)_{ar}$, $\nu(CN)_{ar}$	14
1117 s	1116 s	1118 w	1218	73.90	1112 s	1112 m	1110 w	1210	56.15	1107 m	1110 m	1106 w	1209	58.33	$\nu(CC)_{ar}$, $\nu(CN)_{ar}$	13
			1120	22.45				1124	39.88				1121	46.67	$\nu(CC)_{ar}$, $\nu(CN)_{ar}$	
1062 w	1065 w	1068 s			1065 w	1065 w	1068 vs			1065 w	1068 w	1068 s			$\nu(CC)_{ar}$, $\nu(CN)_{ar}$	
983 vw	1001 w		1082	3.58	993 vw	1000 vw	987 vw	1088	2.95		1001 w	983 vw	1088	2.46	$\beta(CH)_{ar}$	18b
			987	0.01				965	0.21				956	0.33	$\gamma(CH)_{ar}$	5
		894 w	908	48.89				887	30.42				885	22.56	Ring def	
879 w	889 w	875 vw	887	8.62	885 m	887 m	886 w	864	7.77	881 m	878 w	882 m	862	5.83	$\gamma(CH)_{ar}$, $\gamma(NH)_{ar}$	11
840 m	843 m	842 s	877	11.76	839 m	838 m	842 s	845	66.27	827 m	827 m	830 s	837	56.64	β_sCOO^-	
787 m	787 m	788 w	848	12.76	792 w	790 w	796 vw	844	13.79	795 m		799 w	848	23.09	$\gamma(CH)_{ar}$, $\gamma(NH)_{ar}$	
															βCO	
			764	9.75				751	9.41	701 m			753	8.73	$\varphi(CC)_{ar}$, $\gamma(CH)_{ar}$	4
745 m	746 m	749 w	762	45.40	741 m	741 m	744 w	748	39.52	741 m	739 m	742 w	744	32.11	γ_sCOO^-	
657 w	651 w	651 w	652	55.91	649 w	646 w	649 m	660	2.33	633 m	643 w	645 w	653	2.87	α(CCC)	1
															γ(CO), γ(OH)	
566 m		558 w	601	1.78	606 w		607 w	608	3.10	599 w		599 vw	607	2.34	$\varphi(CC)_{ar}$, $\gamma(CH)_{ar}$	16a
					537 m		535 w									6a

Table 4 continued

2,3-Pyrazinedicarboxylate

Lithium					Sodium					Potassium						
IR KBr	IR ATR	Raman	IR theoret	Inten	IR KBr	IR ATR	Raman	IR theoret	Inten	IR KBr	IR ATR	Raman	IR theoret	Inten		
470 m		460 w	521	3.89				522	21.60	489 w			537	17.17	$\beta_{as}COO^-$	
439 w			446	26.27	438 s		435 m	442	23.62	419 m		411 m	431	26.67	$\varphi(CC)_{ar}$	16b

2,3-Pyrazinedicarboxylate

Rubidium			Cesium				
IR KBr	IR ATR	Raman	IR KBr	IR ATR	Raman		
3059 sh		3064 vs	3054 sh		3058 vs	$\nu(CH)_{ar}$	20b
1619 vs	1626 m	1608 w	1613 vs	1612 m	1604 w	$\nu_{as}COO^-$	
1588 vs	1585 vs		1592 vs	1590 s		$\nu_{as}COO^-$	
				1573 vs		$\nu(CC)_{ar}$, $\nu(CN)_{ar}$	8a
	1566 sh	1559 m		1558 s	1556 m	$\nu(CC)_{ar}$, $\nu(CN)_{ar}$	8b
		1530 s		1531 w	1530 s	$\nu(CC)_{ar}$, $\nu(CN)_{ar}$, $\beta(CH)_{ar}$	19a
1432 s	1436 s	1440 vs	1432 s	1432 s	1436 vs	$\nu(CC)_{ar}$, $\nu(CN)_{ar}$, $\beta(CH)_{ar}$	19b
1389 s	1391 m	1392 m	1388 s	1389 m	1388 m	$\nu_{sym}COO^-$	
1354 s	1354 s	1363 m	1354 s	1351 vs	1361 m	$\nu_{sym}COO^-$	
1201 w	1205 m	1210 m	1201 m	1199 m	1208 m	$\beta(CH)_{ar}$, $\nu(CC)_{ar}$, $\nu(CN)_{ar}$	9a
1160 m	1167 w	1156 w	1160 m	1165 m	1156 w	$\beta(CH)_{ar}$, $\nu(CC)_{ar}$, $\nu(CN)_{ar}$	18a
				1129 vw		$\nu(CC)_{ar}$, $\nu(CN)_{ar}$,	14
1109 m	1109 m	1110 vw	1109 m	1106 s	1106 w	$\nu(CC)_{ar}$, $\nu(CN)_{ar}$	13
1065 w	1066 w	1069 vs	1066 w	1065 w	1069 vs	$\nu(CC)_{ar}$, $\nu(CN)_{ar}$	
	1003 w	1023 vw		1003 vw	1002 vw	$\beta(CH)_{ar}$	18b
881 m	885 m	884 m	881 m	881 m	882 m	$\gamma(CH)_{ar}$, $\gamma(NH)_{ar}$	11
828 m	831 m	836 s	827 m	831 m	834 m	β_sCOO^-	
796 w	797 w	798 w	796 w	796 w	796 w	$\gamma(CH)_{ar}$, $\gamma(NH)_{ar}$	
741 m	738 w	747 vw	739 m	734 m	738 w	γ_sCOO^-	
642 w	647 w	643 m	642 w	645 w	645 m	$\alpha(CCC)$	1
564 w		553 w	566 w		557 vw	$\varphi(CC)_{ar}$, $\gamma(CH)_{ar}$	16a
491 w			494 w			$\beta_{as}COO^-$	
422 m		429 m	421 m		425 m	$\varphi(CC)_{ar}$	16b

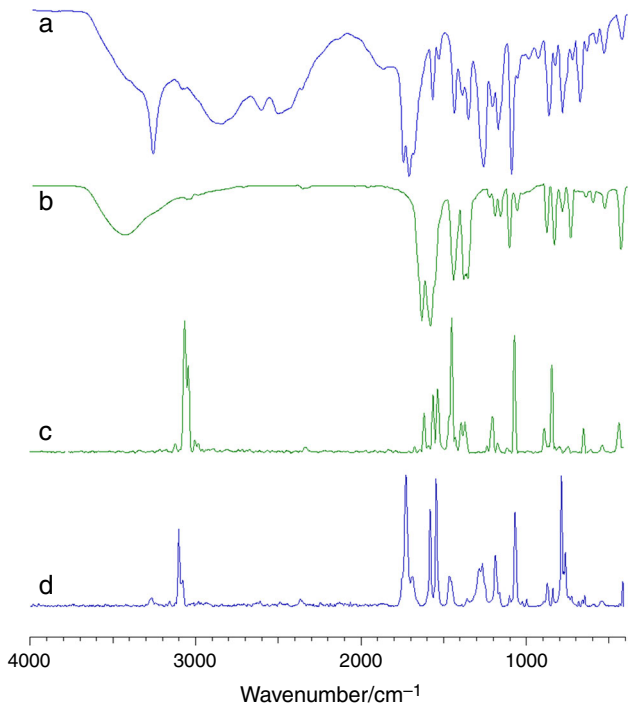

Fig. 3 IR_{KBr} (**a**, **b**) and Raman (**c**, **d**) spectra for 2-pyrazinecarboxylic acid (**a**, **d**) and sodium 2-pyrazinecarboxylate (**b**, **c**)

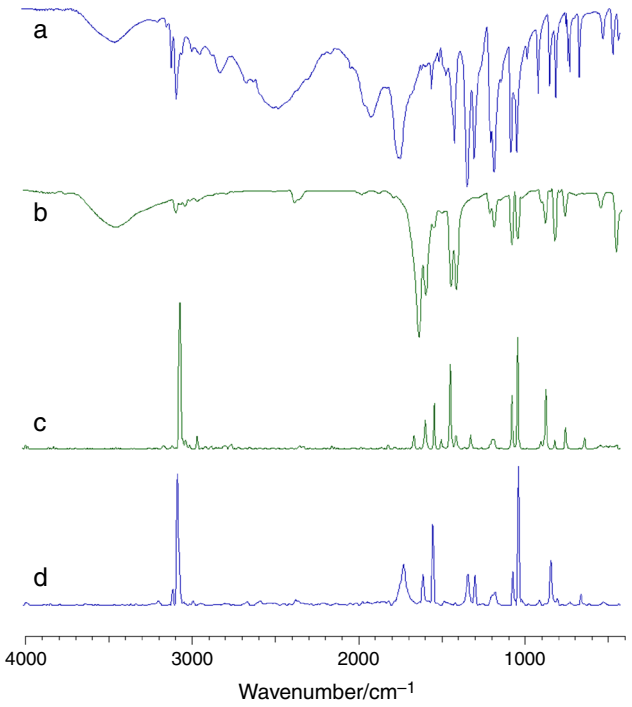

Fig. 4 IR_{KBr} (**a**, **b**) and Raman (**c**, **d**) spectra for 2,3-pyrazinedicarboxylic acid (**a**, **d**) and sodium 2,3-pyrazinedicarboxylate (**b**, **c**)

intensity of the bands derived from the aromatic system and its shift toward lower wavenumbers in the IR and Raman spectra of the salts, compared to the spectrum of acid result from the decreased force constants and polarization of C–H and C–C chemical bonds in the ring. This is related to the perturbation of the electron charge distribution in the aromatic ring of the ligand upon the interaction of the alkali metal with the carboxyl group. From our previous works [57, 59, 60], it follows that the alkali metals disturb the electron system of the aromatic ring in a number of ligands, e.g., benzoic, salicylic and pyridinecarboxylic acids, as well as acids containing five-membered heterocyclic rings.

In the IR_{KBr}, IR_{ATR} and Raman spectra of 2-pyrazinecarboxylates, as compared with the acid, one observes a disappearance of the band 7b associated with the vibration of the CH groups of the aromatic ring. The wavenumbers of several bands in the spectra of the salt decrease. These are the bands numbered: 20b, 8a, 8b, 19a, 19b, 18b, 6b, 16b (in the IR_{KBr} spectra), 20b, 8b, 19b, 5, 11, 6a, 6b (in the IR_{ATR} spectra) and 20a, 8a 8b, 19b, 11, 6b, 16b (in the Raman spectra). It was also observed that the wavenumbers of some bands derived from the vibration of the aromatic ring increase in the salts, compared to the spectrum of the ligand. These bands are: 20a, 9a, 14, 13, 18a (in the IR_{KBr} spectra), 20a, 13, 18a (in the IR_{ATR} spectra) and 14, 18a (in the Raman spectra). The IR_{KBr}, IR_{ATR} and Raman spectra of the salts there occurred a deformation vibration band of the aromatic ring (labeled 4), which was absent in the spectrum of the acid. In the Raman spectra of the salts appeared bands marked with numbers 19a and 6a, which were not observed in the spectrum of the acid.

In the studied series of the alkali metal salts of 2-pyrazinecarboxylate, wavenumbers of many aromatic ring bands decrease regularly in the order Li–Na–K–Rb–Cs. These include the bands 8a, 8b, 19a, 19b, 9a, 18a (in the IR_{KBr} and IR_{ATR} spectra) and 8a, 19b, 18a (in the Raman spectra). Based on the analysis of changes in the wavenumber ranges of an aromatic ring of 2-pyrazinecarboxylate, and salts thereof it can be concluded that alkali metals disturb the electronic system of the acid, and that the degree of perturbation increases in the studied series in the order Li–Na–K–Rb–Cs.

As compared to the free acid, in the spectra of the salt of 2,3-pyrazinedicarboxylate multiple bands derived from the vibration of the aromatic ring disappeared. These bands are indicated by numbers: 20a, 8a, 8b, 19a, 6a, 18b, 5, 4 (in the IR_{KBr} spectra), 20a, 8a, 5, 4 (in the IR_{ATR} spectra) and 20a, 8a, 4, 6 (in the Raman spectra). Observed was a decrease in the wavenumbers of an aromatic ring vibration. These bands are indicated by numbers: 9a, 18a, 1 (in the IR_{KBr} spectra), 8b, 19a, 9a, 18a, 14, 1 (in the IR_{ATR} spectra) and 20b, 8b, 19a, 18a, one (in the Raman spectra).

Wavenumber of some vibrations of the aromatic ring increased in salts with respect to the ligand (lane 13 and 11 present in the IR_{KBr}, IR_{ATR} and Raman spectra).

Changes in the aromatic ring vibration wavenumbers in the studied series of 2,3PDCA acid salts occur irregularly in the direction Li–Cs. In general, in instances of salts with monocarboxylic acids, these changes are regular in the series Li–Na–K–Rb–Cs (for example: 2-pyrazinecarboxylate [this work], 2-pyridinecarboxylates [48], 3-pyridinecarboxylates and 4-pyridinecarboxylates [47]. Based on changes in wavenumber and intensity of the aromatic ring vibration bands in the salts as compared to the ligand, it can be concluded that alkali metals disturb the electron charge distribution in the aromatic ring of 2,3-pyrazinedicarboxylic acid. The effect of alkali metals on the electron charge distribution (decrease in the charge distribution) in the pyrazine ring is much greater in the case of a dicarboxylic acid salt (2PCA) than for the monecarboxylate acid (2,3PDCA).

NMR study

Chemical shifts of the proton signals in ^{1}H NMR spectra of alkali metal 2-pyrazinecarboxylates (H2: 8.90–9.01, H3: 8.45–8.62, H4: 8.29–8.54) display lower values than those for acids (values: H2: 9.19, H3: 8.84, H4: 8.79) (Table 5). Pyrazine aromatic ring system is disturbed due to the changes in the electron density around the protons of the aromatic ring upon substituting the alkali metal atom to the carboxyl group of the acid. Chemical shift values decrease toward Li–Na–K–Rb. In the case of cesium salt, the mentioned values are similar to those of the sodium salt. A ^{1}H NMR spectrum was registered for 2,3-pyrazinedicarboxylate and its lithium salt. The spectra of the other salts of 2,3-pyrazinedicarboxylate were not registered, due to the very poor solubility of these salts in the available solvents. A comparison of the spectra of 2,3-pyrazinedicarboxylate and its lithium salt implies that lithium disturbs the aromatic ring charge distribution (Table 6). Proton

Table 5 Values of the chemical shifts [ppm] in the spectra of ^{1}H and ^{13}C NMR of 2-pyrazinecarboxylic acid (2-PCA) and its salts determined experimentally and by a theoretical GIAO/B3LYP/6-311++G** method

	2PCA	2-Pyrazinecarboxylate				
		Lithium	Sodium	Potassium	Rubidium	Cesium
^{1}HNMR						
H2						
Exp.	9.19	9.08	8.94	8.90	8.91	8.95
Theoret.	8.69	9.74	9.73	9.71	–	–
H3						
Exp.	8.84	8.62	8.48	8.45	8.47	8.50
Theoret.	8.71	8.75	8.68	8.63	–	–
H4						
Exp.	8.79	8.54	8.29	8.41	8.43	8.47
Theoret.	8.83	8.67	8.57	8.52	–	–
^{13}CNMR						
C1						
Exp.	143.89	142.75	143.12	142.99	142.88	143.15
Theoret.	164.99	151.98	153.86	154.95	–	–
C2						
Exp.	145.52	145.18	144.94	144.85	144.84	144.96
Theoret.	171.40	153.54	153.76	153.41	–	–
C3						
Exp.	144.58	144.77	143.36	143.07	143.02	143.36
Theoret.	170.61	151.41	150.33	149.57	–	–
C4						
Exp.	147.68	151.05	153.37	153.97	154.12	153.23
Theoret.	165.89	148.87	148.63	148.24	–	–
C5						
Exp.	165.09	166.16	166.29	166.14	166.13	166.25
Theoret.	187.90	186.16	179.96	179.67	–	–

Table 6 Values of the chemical shifts [ppm] in the spectra of ^{1}H and ^{13}C NMR of 2-pyrazinedicarboxylic acid (2,3PDCA) and its salts determined experimentally and by a theoretical GIAO/B3LYP/6-311++G** method

	2,3PDCA	2,3-Pyrazinedicarboxylate		
		Lithium	Sodium	Potassium
^{1}HNMR				
H3				
Exp.	8.85	8.27	–	–
Theoret.	8.73	8.58	8.60	8.57
H4				
Exp.	8.85	8.27		
Theoret.	8.78	8.61	7.69	7.73
^{13}CNMR				
C1				
Exp.	145.23	140.95	–	–
Theoret.	144.42	165.91	151.56	154.06
C2				
Exp.	145.23	140.95	–	–
Theoret.	158.43	144.82	169.53	169.99
C3				
Exp.	145.59	151.42	–	–
Theoret.	158.87	145.28	151.17	150.37
C4				
Exp.	145.59	151.42	–	–
Theoret.	148.36	151.05	139.28	138.18
C5				
Exp.	165.97	169.70	–	–
Theoret.	169.86	182.66	169.61	171.51
C6				
Exp.	165.97	169.70	–	–
Theoret.	170.42	187.43	179.91	178.70

chemical shift values (in experimental 1HNMR spectra for lithium 2,3-pyrazinedicarboxylate: H3, H4: 8.85) are lower in salt than in acid (H3, H4: 8.27). Theoretical calculations show that in the case of sodium and potassium salts chemical shift values are also lower than the corresponding chemical shifts for protons in the ligand. It is therefore concluded that the alkali metals disturb the electron system of the aromatic ring of 2,3-pyrazinedicarboxylate. Effect of alkali metals on the electronic charge distribution is higher in the case of 2,3-pyrazinecarboxylate. Changes in the chemical shifts of protons in the salts of a ligand are greater for 2,3-pyrazinedicarboxylates than 2-pyrazinecarboxylates. This is evidenced both by chemical shift values that were determined experimentally and those theoretically calculated.

After substituting the alkali metal atom in the carboxyl group of 2-pyrazinecarboxylate a slight increase can be seen in chemical shifts of carbon of the carboxyl group in

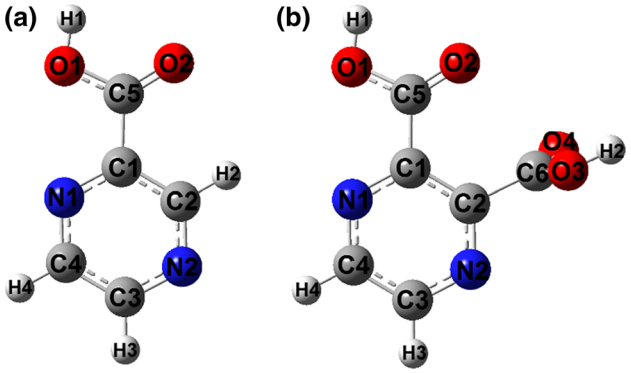

Fig. 5 Numbering of the atoms in the 2-pyrazinecarboxylic acid (**a**) and 2,3-pyrazinedicarboxylic acid (**b**)

the ^{13}C NMR spectra due to the decrease in the electron density around the carbon atom of the carboxyl group. Much more pronounced changes were observed in the chemical shifts of atoms of an aromatic ring. In the 2-pyrazinecarboxylates, the electron density on the carbon atoms numbered C1, C2, and C3 (Fig. 5a) increases in relation to that of the ligand, what is observed as a decrease in the chemical shifts in the spectra of ^{13}C-NMR. The electron density at the C4 atom decreases—an increase is observed in ^{13}C chemical shift values in the salts in relation to the acid. Changes in chemical shifts of carbons for 2-pyrazinecarboxylates of alkali metals with respect to 2-pyrazinecarboxylic acid indicate that alkali metals disturb the electron charge distribution in the aromatic ring of the ligand. An increase in the perturbation of the electron charge distribution was observed along the series Li–Na–K–Rb. A comparison of the chemical shifts in the spectra of ^{13}C-NMR implies that the effect of cesium on the electron charge distribution of 2-pyrazinecarboxylic acid is similar to that of sodium (similar chemical shifts in the salts of sodium and cesium), which was confirmed by the proton spectra of the studied compounds.

Significant changes in the chemical shifts of carbons in the ^{13}C NMR spectrum were observed in the case of lithium substitution to the carboxyl groups of 2,3-pyrazinedicarboxylate. The values of the chemical shifts of atoms indicated C1 and C2 (Fig. 5b) decrease (indicating an increase in the electron density) and the remaining atoms of the aromatic ring increase (decrease in electron density). Changes in chemical shifts of carbons in the NMR spectra of the salt with respect to the ligand calculated theoretically are greater for alkali metal 2,3-pyrazinedicarboxylates than for 2-pyrazinecarboxylates.

Aromaticity and NBO analysis

Upon the substitution of the alkali metal atom to the carboxylic group of 2-pyrazinecarboxylic, and 2,3-

Table 7 Aromaticity indices (HOMA, GEO, EN) and Bird's index (I_6) for 2PCA, 2,3PDCA and their salts (lithium, sodium, potassium) (calculated for the structure optimized in B3LYP/6-311++G**)

Aromaticity indices	2PCA	2-Pyrazinecarboxylate			2,3PDCA	2,3-Pyrazinedicarboxylate		
		Li	Na	K		Li	Na	K
HOMA	0.991	0.988	0.990	0.989	0.985	0.969	0.952	0.952
EN	0.003	0.005	0.004	0.004	0.003	0.007	0.010	0.015
GEO	0.006	0.007	0.006	0.007	0.013	0.024	0.039	0.033
I_6	89.44	89.59	88.76	88.62	90.31	90.11	86.85	84.95

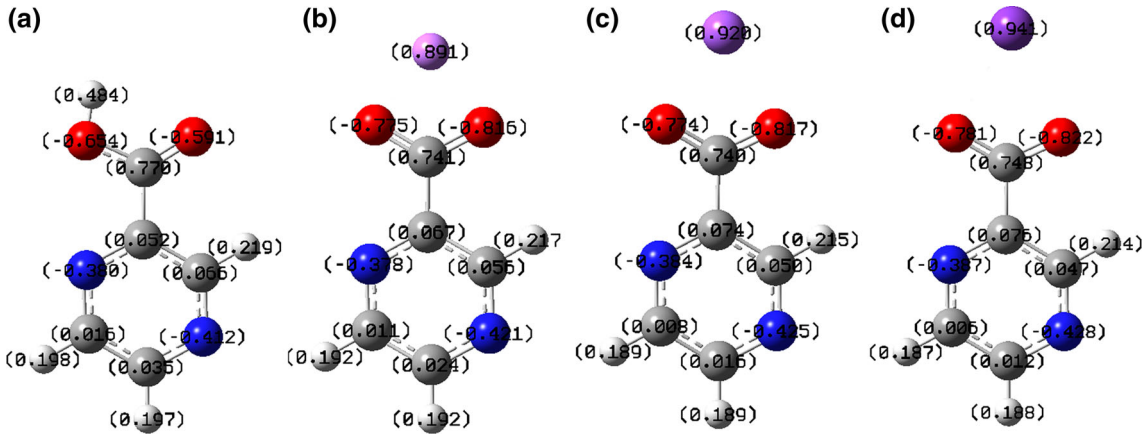

Fig. 6 Electron charge distribution calculated by NBO in B3LYP/6-311++G** for 2-pyrazinecarboxylic (**a**) acid and lithium (**b**), sodium (**c**) and potassium (**d**) 2-pyrazinecarboxylates

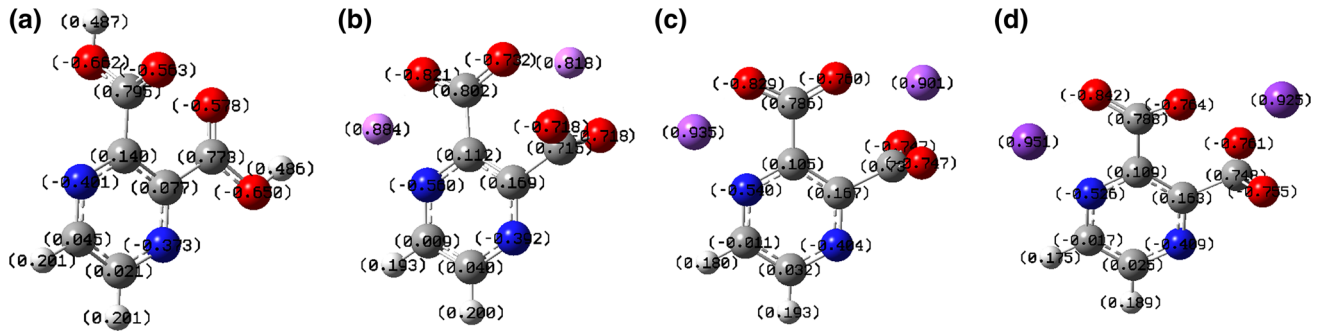

Fig. 7 Electron charge distribution calculated by NBO in B3LYP/6-311++G** for 2,3-pyrazinedicarboxylic acid (**a**) and lithium (**b**), sodium (**c**) and potassium (**d**) 2,3-pyrazinedicarboxylates

pyrazinedicarboxylic acids, the aromaticity of the pyrazine ring decreased. Calculated HOMA aromaticity indices and Bird's I_6 indices display the lower values for the salt in comparison with the ligands (Table 7). Comparing the ligand of Table 7, we found that alkali metals have much greater impact on the aromaticity change (decrease in the aromaticity index values) of 2,3-pyrazinedicarboxylic acid than of the 2-pyrazinecarboxylic acid.

The values of the electronic charges in ligands (2PCA and 2,3PDCA) and their salts of lithium, sodium and potassium were calculated using NBO (natural bond orbital method). Upon the substitution of the alkali metal atom in the carboxyl group of 2PCA, a change in the charge distribution of electron on the carbon of the carboxyl group and the aromatic ring occurred (Fig. 6). An increase in the value of the electron charge with respect to the carboxylic acid group occurred on the oxygen atoms in the carboxylate anion of salts. A small increase in the value of electron charge was calculated by NBO (B3LYP/6-311++G**), for the nitrogen atoms in the pyrazine ring of 2PCA salts with

respect to that of the ligand. The electronic charge on the carbon atoms No C2, C3 and C4 increases, while it decreases on the C1 atom. The changes in the charge values occur along the 2PCA–Li–Na–K series. The electronic charge on aromatic protons of lithium, sodium and potassium 2-pyrazinecarboxylates increases as compared with the ligand. Similar changes were observed in the experimental ^{1}H-NMR spectra—chemical shifts were reduced in a series 2PCA–Li–Na–K–Rb–Cs, which implies the increasing values of electron density on the aromatic protons.

The electronic charge on nitrogen atoms in the pyrazine ring in lithium, sodium and potassium 2,3-pyrazinedicarboxylate increases significantly with respect to the ligand (Fig. 7). The values of electronic charge on the aromatic ring carbons of the 2,3PDCA salts also vary from the value for the ligand. These changes in the alkali metal 2,3-pyrazinedicarboxylates are greater than in the 2-pyrazinecarboxylates.

Conclusions

On the basis of experimental and theoretical calculations, it was found that:

1. Comparing the curves of the thermal decomposition of the alkali metal salt of studied acids one can conclude that salts of 2-pyrazinecarboxylic acid have a higher thermal stability than the salts of 2,3-pyrazinedicarboxylate.
2. Spectroscopic (IR, Raman and NMR) data showed that alkali metals disturb the electronic system of the aromatic ring of ligands, (of 2-pyrazinecarboxylate, and 2,3-pyrazinedicarboxylate). The degree of perturbation increases in the studied series salts in order: Li–Na–K–Rb–Cs.
3. Experimental studies showed that alkali metals to much greater extent impact on the electronic charge distribution of 2,3-pyrazinedikarboxylic than of 2-pyrazinecarboxylic acid.
4. Theoretical calculations (aromaticity index values, the charge distribution by NBO) performed for geometrically optimized structures confirm the results of experiments on the effect of alkali metals on the electron charge distribution of ligand.

Acknowledgements This work was supported by Bialystok University of Technology in the frame of funding for statutory research (No. S/WBiIŚ/1/2012). Thermogravimetric research was performed at the Center of Synthesis and Analysis BioNanoTechno of the University of Bialystok. The equipment in the Center of Synthesis and Analysis BioNanoTechno of University of Bialystok was funded by the EU, Project: POPW.01.03.00–20–034/09–00.

References

1. Müller R, Rappert S. Pyrazines: occurrence, formation and biodegradation. Appl Microbiol Biotechnol. 2010;85:1315–20.
2. Wagner R, Czerny M, Bielohradsky J, Grosch W. Structure-odour-activity relationships of alkylpyrazines. Z Für Leb Forsch A. 1999;208:308–16.
3. Hogben CAM, Tocco DJ, Brodie BB, Schanker LS. On the mechanism of intestinal absorption of drugs. J Pharmacol Exp Ther. 1959;125:275–82.
4. Jakoby WB. Metabolic basis of detoxication. Elsevier; 2012.
5. Schanker LS, Shore PA, Brodie BB, Hogben CAM. Absorption of drugs from the stomach I. The rat. J Pharmacol Exp Ther. 1957;120:528–39.
6. Sausville JW, Spoerri PE. Syntheses in the Pyrazine Series. IV. 2-Sulfanilamidopyrazine. J Am Chem Soc. 1941;63:3153–4.
7. Ambrogi V, Bloch K, Daturi S, Logemann W, Parenti M. Synthesis of pyrazine derivatives as potential hypoglycemic agents. J Pharm Sci. 1972;61:1483–6.
8. Khamar BM, Singh C, Modi RI. Hypoglycemic compounds. U.S. Patent No 9,029,56. 2015.
9. Meurer LC, Tolman RL, Chapin EW, Saperstein R, Vicario PP, Zrada MM, et al. Synthesis and hypoglycemic activity of substituted 8-(1-piperazinyl) imidazo [1, 2-a] pyrazines. J Med Chem. 1992;35:3845–57.
10. Yuan K, Ma S, Zhu L, Liu H. Salts of methyl (R)-7-[3-amino-4-(2, 4, 5-trifluoro-phenyl)-butyryl]-3-trifluoromethyl-5, 6, 7, 8-tetrahydro-imidazo [1, 5-A] pyrazine-1-carboxylate. 2013.
11. Bicking JB, Mason JW, Woltersdorf OW Jr, Jones JH, Kwong SF, Robb CM, et al. Pyrazine diuretics. I. N-amidino-3-amino-6-halopyrazinecarboxamides. J Med Chem. 1965;8:638–42.
12. Dolezal M, Zitko J. Pyrazine derivatives: a patent review (June 2012-present). Expert Opin Ther Pat. 2015;25:33–47.
13. Ukrainets I, Bereznyakova N. Heterocyclic diuretics. Chem Heterocycl Compd. 2012;48:1–11.
14. Krátký M, Vinšová J, Novotná E, Stolaříková J. Salicylanilide pyrazinoates inhibit in vitro multidrug-resistant Mycobacterium tuberculosis strains, atypical mycobacteria and isocitrate lyase. Eur J Pharm Sci. 2014;53:1–9.
15. Kushner S, Dalalian H, Sanjurjo J, Bach F Jr, Safir S, Smith V Jr, et al. Experimental chemotherapy of tuberculosis. II. The synthesis of pyrazinamides and related compounds1. J Am Chem Soc. 1952;74:3617–21.
16. Foks H, Balewski L, Gobis K, Dabrowska-Szponar M, Wisniewska K. Studies on pyrazine derivatives LII: antibacterial and antifungal activity of nitrogen heterocyclic compounds obtained by pyrazinamidrazone usage. Heteroat Chem. 2012;23:49–58.
17. Lima CHS, Henriques GMO, Candea LPA, Lourenco CSM, Bezerra AFMF, Ferreira LM, Kaiser RC, de Souza VNM. Synthesis and Antimycobacterial Evaluation of N′-(E)-heteroaromaticpyrazine-2-carbohydrazide derivatives. Med Chem. 2011;7:245–9.
18. Judge V, Narasimhan B, Ahuja M. A review of biological potential of pyrazinamide derivatives. Hygeia J Drugs Med. 2012;4:1–6.

19. de L. Ferreira M, Candea Andre LP, de O H, Maria das Gracas M, Kaiser CR, da S LCH, de Souza MVN. Synthesis and cytotoxic evaluation of disubstituted n-acylhydrazones pyrazinecarbohydrazide derivatives. Lett Drug Des Discov. 2010;7:275–80.
20. Vergara FM, Lima CH da S, Maria das Graças M de O, Candéa AL, Lourenço MC, Ferreira M de L, Kaiser RC, de Souza VNM. Synthesis and antimycobacterial activity of N′-[(E)-(monosubstituted-benzylidene)]-2-pyrazinecarbohydrazide derivatives. Eur J Med Chem 2009;44:4954–9.
21. Sigroha S, Narasimhan B, Kumar P, Khatkar A, Ramasamy K, Mani V, et al. Design, synthesis, antimicrobial, anticancer evaluation, and QSAR studies of 4-(substituted benzylidene-amino)-1, 5-dimethyl-2-phenyl-1, 2-dihydropyrazol-3-ones. Med Chem Res. 2012;21:3863–75.
22. Aly AA, Nour-El-Din AM. Functionality of amidines and amidrazones. Arkivoc. 2008;1:153–94.
23. Srivastava K, Purohit S, Singhal S. Studies on nitrogen and sulphur containing heterocyclic compound: 1, 3, 4-thiadiazole. Asian J Biomed Pharm Sci 2013; 3:6.
24. Zhang Z, Wei T, Hou J, Li G, Yu S, Xin W. Tetramethylpyrazine scavenges superoxide anion and decreases nitric oxide production in human polymorphonuclear leukocytes. Life Sci. 2003;72:2465–72.
25. Feng L, Ke N, Cheng F, Guo Y, Li S, Li Q, et al. The protective mechanism of ligustrazine against renal ischemia/reperfusion injury. J Surg Res. 2011;166:298–305.
26. Liu S, Cai Y, Evans TW, McCormack DG, Barer GR, Barnes PJ. Ligustrazine is a vasodilator of human pulmonary and bronchial arteries. Eur J Pharmacol. 1990;191:345–50.
27. Sun L, Li Y, Shi J, Wang X, Wang X. Protective effects of ligustrazine on ischemia-reperfusion injury in rat kidneys. Microsurgery. 2002;22:343–6.
28. Chen L, Lu Y, Wu J, Xu B, Zhang L, Gao M, et al. Ligustrazine inhibits B16F10 melanoma metastasis and suppresses angiogenesis induced by vascular endothelial growth factor. Biochem Biophys Res Commun. 2009;386:374–9.
29. Jiang F, Qian J, Chen S, Zhang W, Liu C. Ligustrazine improves atherosclerosis in rat via attenuation of oxidative stress. Pharm Biol. 2011;49:856–63.
30. Peng W, Hucks D, Priest R, Kan Y, Ward J. Ligustrazine-induced endothelium-dependent relaxation in pulmonary arteries via an NO-mediated and exogenous L-arginine-dependent mechanism. Br J Pharmacol. 1996;119:1063–71.
31. Adams A, De Kimpe N. Formation of pyrazines from ascorbic acid and amino acids under dry-roasting conditions. Food Chem. 2009;115:1417–23.
32. Arnoldi A, Arnoldi C, Baldi O, Griffini A. Flavor components in the Maillard reaction of different amino acids with fructose in cocoa butter-water. Qualitative and quantitative analysis of pyrazines. J Agric Food Chem. 1988;36:988–92.
33. Hawksworth G, Scheline RR. Metabolism in the rat of some pyrazine derivatives having flavour importance in foods. Xenobiotica. 1975;5:389–99.
34. Maga JA. Pyrazine update. Food Rev Int. 1992;8:479–558.
35. Ferreira SB, Kaiser CR. Pyrazine derivatives: a patent review (2008—present). Expert Opin Ther Pat. 2012;22:1033–51.
36. Ura Y, Sakata G, Makino K, Kawamura Y, Ikai T, Oguti T. Quinoxaline derivatives and herbicidal composition. U.S. Patent No. 5,364,831. 1994.
37. Hayes AW. Principles and methods of toxicology [Internet]. [New York]: CRC Press; 2007 [cited 2015 Oct 15]. http://www.crcnetbase.com/isbn/9780849337789.
38. Yumino K, Kawakami I, Tamura M, Hayashi T, Nakamura M. Paraquat-and diquat-induced oxygen radical generation and lipid peroxidation in rat brain microsomes. J Biochem (Tokyo). 2002;131:565–70.
39. Nakamura A, Ataka T, Segawa H, Takeuchi Y, Takematsu T. Structure-activity relationship of herbicidal 2, 3-dicyano-5-substituted pyrazines. Agric Biol Chem. 1983;47:1555–60.
40. Doležal M, Kráľová K. Synthesis and evaluation of pyrazine derivatives with herbicidal activity. INTECH Open Access Publisher; 2011.
41. Jackson G, Einsele H, Moreau P, Miguel JS. Bortezomib, a novel proteasome inhibitor, in the treatment of hematologic malignancies. Cancer Treat Rev. 2005;31:591–602.
42. Richardson PG, Sonneveld P, Schuster MW, Irwin D, Stadtmauer EA, Facon T, et al. Bortezomib or high-dose dexamethasone for relapsed multiple myeloma. N Engl J Med. 2005;352:2487–98.
43. Kamal A, Ramakrishna G, Raju P, Rao AVS, Viswanath A, Nayak VL, et al. Synthesis and anticancer activity of oxindole derived imidazo[1,5-a]pyrazines. Eur J Med Chem. 2011;46:2427–35.
44. Rodrigues FA, Bomfim I da S, Cavalcanti BC, do Ó Pessoa C, Pinheiro AC, Lima CH, de Souza VNM. Biological evaluation of pyrazinamide derivatives as an anticancer class. Eur Chem Bull. 2014;3:358–61.
45. Lewandowski W, Kalinowska M, Lewandowska H. The influence of metals on the electronic system of biologically important ligands. Spectroscopic study of benzoates, salicylates, nicotinates and isoorotates. Review. J Inorg Biochem. 2005;99:1407–23.
46. Lewandowski W, Fuks L, Kalinowska M, Koczoń P. The influence of selected metals on the electronic system of biologically important ligands. Spectrochim Acta A Mol Biomol Spectrosc. 2003;59:3411–20.
47. Koczoń P, Hrynaszkiewicz T, Świsłocka R, Samsonowicz M, Lewandowski W. Spectroscopic (Raman, FT-IR, and NMR) study of alkaline metal nicotinates and isonicotinates. Vib Spectrosc. 2003;33:215–22.
48. Świderski G, Wojtulewski S, Kalinowska M, Świsłocka R, Lewandowski W. Effect of alkali metal ions on the pyrrole and pyridine π-electron systems in pyrrole-2-carboxylate and pyridine-2-carboxylate molecules: FT-IR, FT-Raman, NMR and theoretical studies. J Mol Struct. 2011;993:448–58.
49. Doležal M, Zitko J, Jampílek J. Pyrazinecarboxylic acid derivatives with antimycobacterial activity. 2012.
50. Gaussian09 RA. 1, MJ Frisch, GW Trucks, HB Schlegel, GE Scuseria, MA Robb, JR Cheeseman, G. Scalmani, V. Barone, B. Mennucci, GA Petersson, et al., Gaussian. Inc Wallingford CT. 2009.
51. Beaula TJ, Packiavathi A, Manimaran D, Joe IH, Rastogi V, Jothy VB. Quantum chemical computations, vibrational spectroscopic analysis and antimicrobial studies of 2, 3-Pyrazinedicarboxylic acid. Spectrochim Acta A Mol Biomol Spectrosc. 2015;138:723–35.
52. Rode JE, Dobrowolski JC, Jamróz MH, Borowiak MA. Theoretical IR, Raman and NMR spectra of 1, 2-and 1, 3-dimethylenecyclobutane. Vib Spectrosc. 2001;25:133–49.
53. Reed AE, Weinstock RB, Weinhold F. Natural population analysis. J Chem Phys. 1985;83:735–46.
54. Krygowski TM, Cyrański M. Separation of the energetic and geometric contributions to the aromaticity. Part IV. A general model for the π-electron systems. Tetrahedron. 1996;52:10255–64.
55. Bird C. A new aromaticity index and its application to five-membered ring heterocycles. Tetrahedron. 1985;41:1409–14.
56. Varsányi G. Vibrational spectra of benzene derivatives. Oxford: Elsevier; 2012.
57. Lewandowski W, Świderski G, Świslocka R, Wojtulewski S, Koczoń P. Spectroscopic (Raman, FT-IR and NMR) and theoretical study of alkali metal picolinates. J Phys Org Chem. 2005;18:918–28.
58. Świsłocka R, Regulska E, Samsonowicz M, Lewandowski W. Experimental (FT-IR, FT-Raman, 1 H, 13 C NMR) and theoretical study of alkali metal 2-aminonicotinates. Polyhedron. 2009;28:3556–64.

59. Kalinowska M, Siemieniuk E, Kostro A, Lewandowski W. The application of A j, BAC, I 6, HOMA indexes for quantitative determination of aromaticity of metal complexes with benzoic, salicylic, nicotinic acids and benzene derivatives. J Mol Struct Theochem. 2006;761:129–41.

60. Kalinowska M, Świsłocka R, Borawska M, Piekut J, Lewandowski W. Spectroscopic (FT-IR, FT-Raman, UV) and microbiological studies of di-substituted benzoates of alkali metals. Spectrochim Acta A Mol Biomol Spectrosc. 2008;70:126–35.